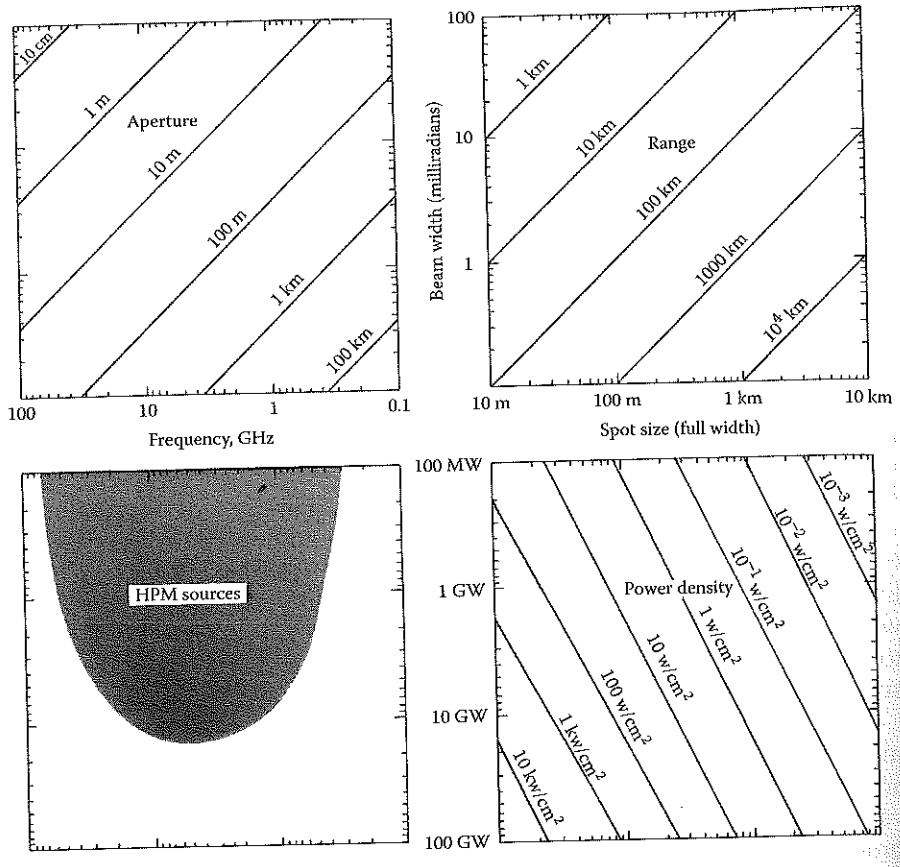

FIGURE 3.9
Nomograph for estimating mission parameters.

(2) Assuming that platform constraints limit ERP and antenna diameter, one deduces a power density that can be incident on a target at the required range. This puts the requirement on the effects (e.g., by tailoring waveforms or properly choosing frequencies) at the power density that technology can practically produce. This line of reasoning has led to the medium power microwave program described previously. This logic accepts the realities of technology and that new platforms are unlikely to be created exclusively for HPM, and places an emphasis on reducing the lethality threshold by increasing the sophistication of the attack.

Figure 3.10 shows another form of nomograph for DEW or power beaming.

3.2.5 Electromagnetic Terrorism

Complex systems such as government, industry, and the military cannot function without fast information flow. The West's data and communications

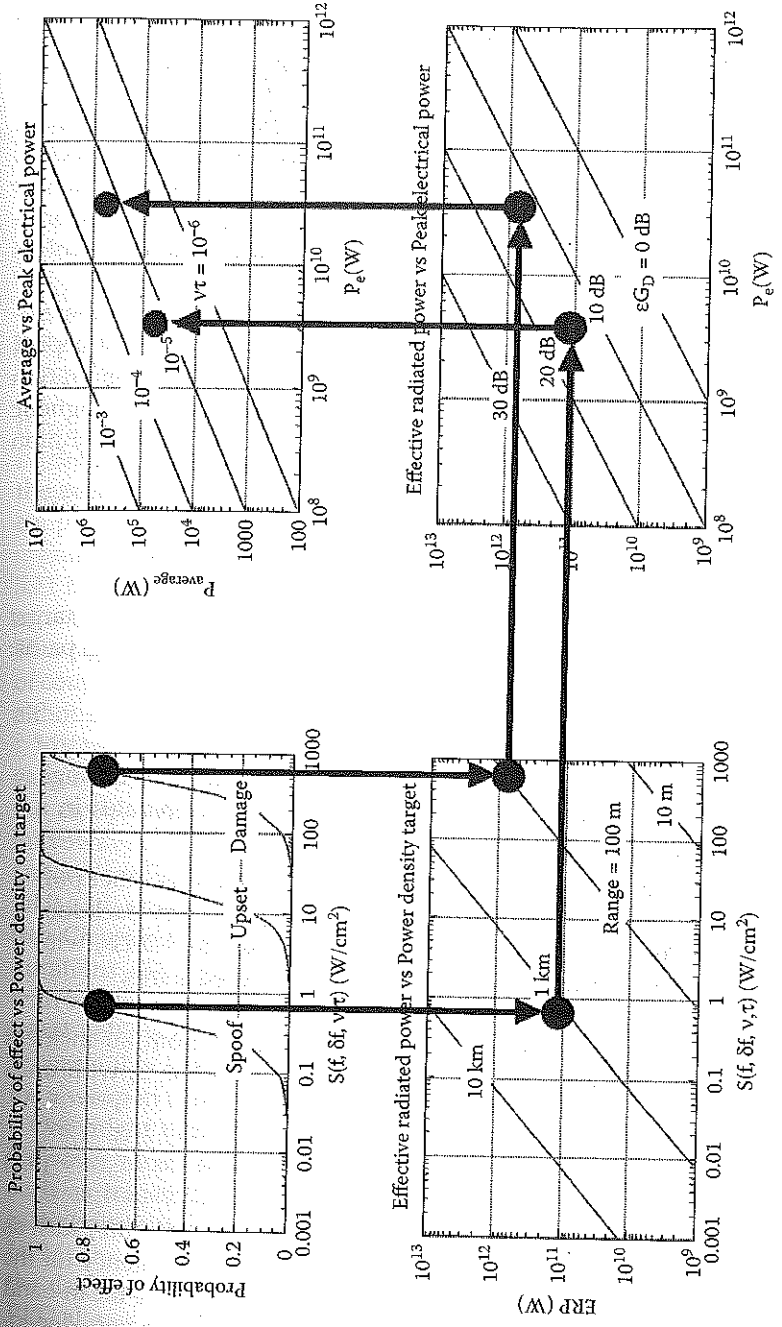

FIGURE 3.10
Another DEW nomograph. Choosing a high probability of effect for either spoofing or damage, and range for attack, gives ERP. Then choosing antenna gain gives peak power. Finally, choosing duty factor determines average power.

infrastructure will remain a soft electromagnetic target in the foreseeable future. That is because no one wants to pay for it. (*Soft kill* will inhibit or degrade the function of a target system leaving the target system electrically and physically intact. *Hard kill* will damage or destroy the target system.) This is a fundamental and growing EM infrastructure vulnerability; it can be exploited.

The technology is increasingly available and inexpensive. For example, see the DS110 in Figure 6.13. The vulnerability of infrastructure is suspected, but not widely known. Potential targets vary from small systems, such as individual automobiles, to the highly complex (aircraft on takeoff and landing, electrical power grid, oil and gas pipelines, banking, financial centers such as stock markets).

In Russia, former Soviet laboratories have suffered. Their extensive microwave and pulse power technology can be and is being sold to and copied by Third World nations or even terrorists. So far no counterproliferation regimes exist. Should treaties arise to limit proliferation of electromagnetic weapons, they would be virtually impossible to enforce, given the common availability of the technology.

3.2.6 Coupling

Whatever the mode of attack, microwave energy can propagate to the target system internal electronics through two generic types of coupling paths: *frontdoor coupling* and *backdoor coupling*.

- *Frontdoor* denotes coupling through intentional receptors for electromagnetic energy such as antennas and sensors; power flows through transmission lines designed for that purpose and terminates in a detector or receiver.
- *Backdoor* denotes coupling through apertures intended for other purposes or incidental to the construction of the target system. Backdoor coupling paths include seams, cracks, hatches, access panels, windows, doors, and unshielded or improperly shielded wires.

In general, the power coupled to internal circuitry P from an incident power density S is characterized by a coupling cross section S, with units of area:

$$P = S\,\sigma \tag{3.4}$$

For frontdoor paths, σ is usually the effective area of an aperture, such as an antenna or slot. The effective area peaks at the in-band frequency for the antenna and falls off sharply with frequency as roughly f^{-2} above the in-band frequency and f^4 below it. These are only very general relations, very dependent upon mismatch effects and construction details. Therefore, to gain entry

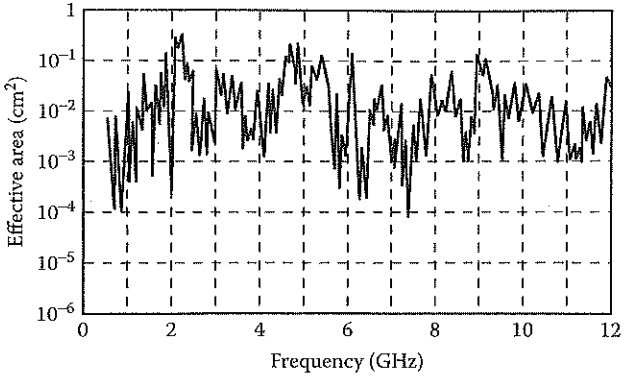

FIGURE 3.11
Typical cross section for coupling into the interior of an object through backdoor channels.

through an antenna, one wants to operate at the in-band frequency if it can be determined. The above discussion is for irradiation into the main lobe of the antenna. Radiating at random angles or in the sidelobes will reduce the coupled power substantially (see Problem 4).

Entering through a backdoor coupling path has many complexities. Figure 3.11 illustrates a general result: the rapid variation of coupling cross section as a function of frequency due to the overlapping sets of coupling paths. This occurs quite generally for backdoor attacks. Therefore, the cross section of coupling is difficult to predict for a specific object without detailed testing, although properties averaged over frequency bands can be predicted.

Microwaves directly couple into equipment through ventilation holes, gaps between panels, and poorly shielded interfaces because apertures into the equipment behave much like a slot in a microwave cavity, allowing microwaves to enter and excite the cavity. Electronic equipment cavity Q factors (see Equation 4.88) are in the range of Q ~ 10, so the time it takes to fill it with energy is about 10 cycles. This is one reason that mesoband pulses (see Chapter 6), which last only a few cycles, can be effective: their pulse durations allow cavities to fill, then end. A general approach for dealing with wiring- and cabling-related backdoor coupling is to determine a known lethal voltage level, and then use this to find the required field strength to generate this voltage. Once the field strength is known, the effective range for a weapon can be calculated.

One might think that one of the most attractive targets for HPM is radar. However, most radar sets are designed with *receiver protection devices* (RPDs), such as transmit/receive switches, to prevent near-field reflections of the radar transmitter from damaging the receiver. RPDs could also protect against HPM. The RPD triggers and strongly attenuates incoming signals that exceed the damage threshold of downstream elements, such as mixers. The typical RPD allows an early spike to propagate through the system and then shorts the remainder of the pulse. The duration and intensity of the spike leakage

are crucial to being able to burn out the more sensitive diodes of the downstream receiver. The technology of the devices used to limit the pulse semiconductors — gas plasma discharge devices, multipacting devices, and ferrite limiters, as well as hybrids and combinations of these devices — is very well developed. However, much fielded hardware has far simpler, older RPD technology, and in some cases this technology is downgraded or removed in the field to facilitate system operation. Attacks against specific systems will require system testing. Short, high power pulses are better for this attack.

It is important in discussions of HPM DEW missions to understand effects nomenclature. *Susceptibility* occurs when a system or subsystem experiences degraded performance when exposed to an EM environment. Electromagnetic *vulnerability* is when this degradation is sufficient to compromise the mission. *Survivability* occurs when the system is able to perform a mission, even in a hostile environment, and *lethality* occurs when a target is incapable of performing its mission after being irradiated.

Most of the effort within the U.S. military research and development community is on lethality, while in the rest of the world it is on survivability.

3.2.7 Hardening

HPM is susceptible to shielding or *hardening* as a countermeasure. Electromagnetic hardening can reduce the vulnerability of a target substantially without the attacker realizing that hardening has been employed. Hardening is produced by control of the entry paths for radiation into the target system and by reduction of the susceptibility of subsystems and the components to which radiation can couple. The drawback of hardening is that it may degrade the target system response and even increase its weight and volume. Moreover, the retrofit cost may be an excessive penalty.

The most effective method is to wholly contain the equipment in a *Faraday cage*, an electrically conductive enclosure, so that HPM cannot penetrate into the equipment. However, most such equipment must communicate with and be fed with power from the outside world, and this can provide entry points via which electrical transients may enter the enclosure and effect damage. While optical fibers address this requirement for transferring data in and out, electrical power feeds remain an ongoing vulnerability.

Shielding electronics by equipment chassis provides only limited protection, as any cables running in and out of the equipment will behave very much like antennas, in effect guiding the high-voltage transients into the equipment.

A low-frequency weapon will couple well into a typical wiring infrastructure, as most telephone lines, networking cables, and power lines follow streets, building risers, and corridors. In most instances, any particular cable run will comprise multiple linear segments joined at approximately right angles. Whatever the relative orientation of the weapons field, more than one linear segment of the cable run is likely to be oriented such that a good coupling efficiency can be achieved.

It is clearly evident that once the defense provided by a transformer, cable pulse arrestor, or shielding is breached, voltages even as low as 50 V can inflict substantial damage upon computer and communications equipment. Items (computers, consumer electronics) exposed to low-frequency, high-voltage spikes (near lightning strikes, electrical power transients) in many instances experience extensive damage, often requiring replacement of most semiconductors in the equipment.

3.2.8 High Power Microwave Effects on Electronics

Once radiation penetrates into the interior of a target system, the susceptibility of the small-scale semiconductor devices, which make up the interior electronics, becomes the key issue in DEW utility. Failures in semiconductor devices due to thermal effects occur when the temperature at the critical junctions is raised above 600 to 800° Kelvin, resulting in changes in the semiconductor up to and including melting. Because the thermal energy diffuses through the semiconductor material, there are several failure regimes, depending upon the duration of the microwave pulse. If the timescale is short compared to thermal diffusion times, the temperature increases in proportion to the deposited energy. It has been established experimentally that semiconductor junction damage depends only upon energy for pulse durations less than 100 nsec, when thermal diffusion can be neglected. Therefore, in this regime the threshold power for damage varies as t^{-1}, as shown in Figure 3.12. For pulses greater than 100 nsec, thermal diffusion carries energy away from the junction. The general result is the *Wunsch–Bell relation*[11] for the power to induce failure:

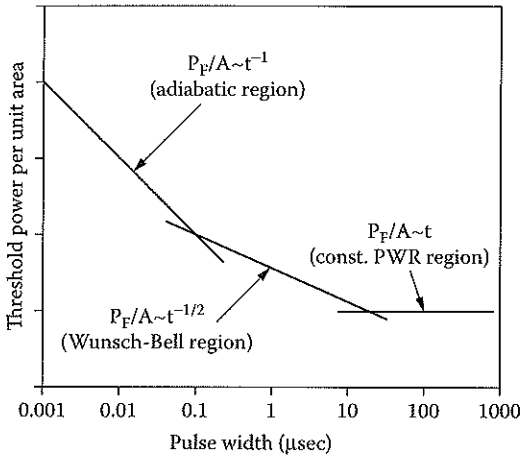

FIGURE 3.12
Power density for burnout vs. pulse width. UWB HPM sources operate in the adiabatic region and narrowband sources in the Wunsch–Bell or constant power regions.

$$P \sim \frac{1}{\sqrt{t}} \tag{3.5}$$

The Wunsch–Bell relation is generally applicable because, even though thermal conductivity and specific heat vary with temperature, these effects cancel out. Therefore, *in the domain between 100 nsec and ~1 msec, the energy required to cause semiconductor junction failure scales as $t^{1/2}$ and the power requirement scales at $t^{-1/2}$*. For pulses longer than ~10 μsec, a steady state occurs in which the rate of thermal diffusion equals the rate of energy deposition. Therefore, the temperature is proportional to power, resulting in a constant power requirement for failure. The energy requirement then scales as t. The consequence of these scaling relations is that the shortest pulses require the highest powers but the least energy. Conversely, the highest energy and lowest power are required for long pulses. UWB HPM sources (Chapter 6) operate in the adiabatic, narrowband sources in the Wunsch–Bell or constant power regions. If energy is to be minimized in deployed weapons, the shorter pulses will be used, and if power is the limiting requirement, then longer pulse durations are indicated.

The above relations apply to single-pulse damage. If there is insufficient time between successive pulses for heat to diffuse, then accumulation of energy or *thermal stacking* will occur. From Figure 3.12, thermal equilibrium occurs in less than 1 msec; therefore, ≳1-kHz repetition rates are required for thermal stacking. The required value of repetition rate will vary with specific targets. There is also the possibility that permanent damage may result from the accumulation of multiple pulses. Some data suggest that gradual degradation occurs even at repetition rates much lower than the rate required for thermal stacking, possibly due to incremental damage. An analogy would be insulator flashover. This effect may allow reductions in the threshold power requirement for electronic damage. Some data indicate that when hundreds to thousands of pulses are used, the damage threshold can be reduced an order of magnitude. Such effects have not been quantified sufficiently. The repetition rate requirement can be relaxed, relative to thermal stacking, and will be determined by mission constraints, such as time on target. In any case, repetitive operation is required for any real engagement, and therefore accumulating damage effects may be inherent in HPM DEW engagements.

Damage is not the only mechanism to consider. *Upset* of digital circuits occurs when HPM couples to the circuit, is rectified at, for example, p-n junctions, and produces voltages equivalent to normal circuit operating voltage.

The development trends of electronic processors have led them to be more susceptible and vulnerable to microwaves. The basic component is the transistor gate, shown in Figure 3.13, which has a working voltage V and junction parasitic capacitance C_p, proportional to the area of the gate. Switching of the transistor occurs by the flow of a current flow of charge $Q = C_pV$ in a

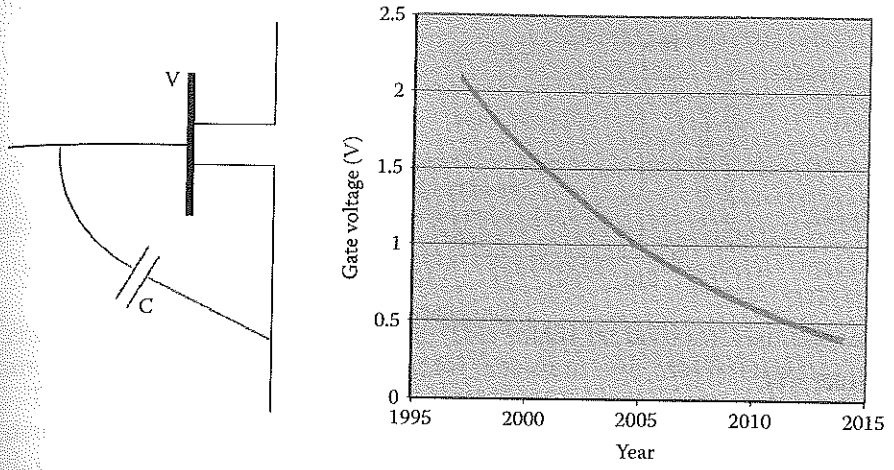

FIGURE 3.13
Circuit of transistor gate and historical trend of gate voltage.

time Δt. The rate of processing, or clock rate, is given by $f = 1/\Delta t$. Power flowing to the transistor is

$$P = VI = VQ/\Delta t = C_pV^2f \tag{3.6}$$

Commercial pressure speeds clock rates, with the result that dissipated power in the gate increases, heating the junction. Such power must be extracted, limiting how dense the gates can be made, which limits processor compactness. Some improvements can be realized by reducing the gate area and hence C_p, but this shrinking of the gates is offset by the need to increase the total number of transistors, and so the dissipated power density remains constant. The attractive way out is to reduce voltage, as $P \sim V^2$. Figure 3.13 shows the continuing fall of voltage, with future declines projected to come. The lowered voltage reduces operating margins, making the circuit more susceptible to noise. This trend makes the chip containing the gates more vulnerable to microwave attack. If a microwave beam falling on the device housing the processor causes high enough voltage at the junction, effects up to burnout of the transistor will occur. Figure 3.14 shows a trend toward lower thresholds for susceptibility as the scale size of integrated circuits is reduced to fit more electronics on single chips.

For classes for commercial off-the-shelf (COTS) equipment, the most common system is the computer. Clock rate as well as the number of transistors is increasing, as the minimum structure size is decreasing with successive computer generations. Figure 3.15 shows effects testing on Pentium III processor-based PCs.[12] The electric field for the onset of effects is given. There is substantial scatter in effects data because of the complex sequence of penetrating the system and computer housing, and the various chassis prop-

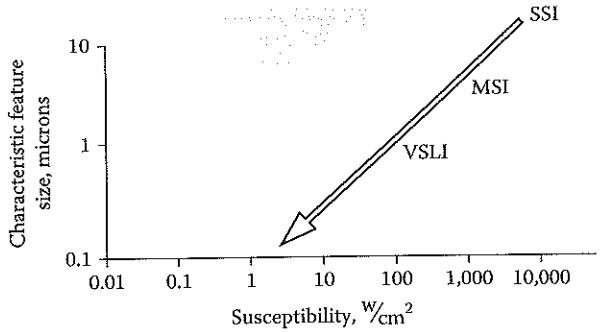

FIGURE 3.14
Feature size of chip technologies falls, lowering the threshold for HPM effects.

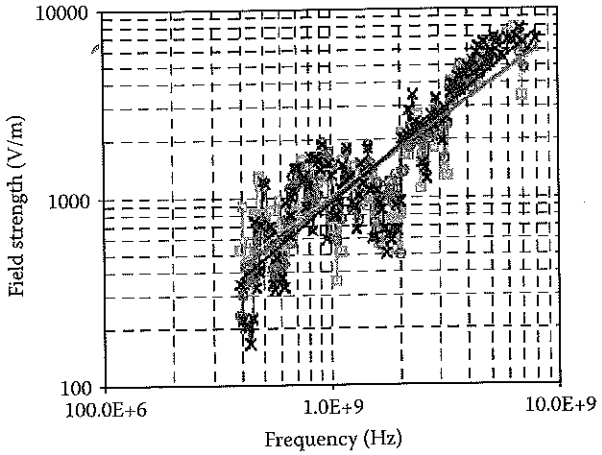

FIGURE 3.15
Electric field strength at which first breakdown effects occur in three Pentium III 667-MHz computers. (Reprinted from Hoad, R., *IEEE Trans. Electromag. Compatibility*, 46, 392, 2004 [Figure 3]. By permission of IEEE.)

agation paths combined with the inherent statistical nature of electronics effects. The system is more vulnerable at lower frequencies, which is a general result for COTS electronics. It is easier to produce effects at lower frequencies when the system is relatively open and has lots of wires. So cable effects dominate below 1 GHz for computers with power cords and wiring. Openings such as slots are more important at higher frequencies. In general, in-band radiation is highly effective at entering and causing severe problems if there is an operating frequency in the microwave. However, the ease of backdoor penetration and the susceptibility of modern digital electronics make this mechanism more likely in COTS systems. However, modern high-speed computers are harder than their predecessors. But when they do fail, the effects are more severe. The most common failure mode is computer

TABLE 3.1
Categories and Consequences of Electronic Effects

Failure Mode	Power Required	Wave Shape	Recovery Process	Recovery Time
Interference/disturbance	Low	Repetitive pulse or continuous	Self-recovery	Seconds
Digital upset	Medium	Short pulse, single or repetitive	Operator intervention	Minutes
Damage	High	UWB or narrowband	Maintenance	Days

crash with manual restart required. This might be because manufacturers are getting smarter about shielding for emissions and interference.

Table 3.1 shows in general the categories of consequences of effects. It demonstrates that the recovery time can vary from seconds to hours. Some think this a major advantage of HPM, obtaining a variety of effects from a single source.

In Europe, effects work concentrates on understanding electronics failure mechanisms to harden their electronics. It is well coordinated between the universities, the electromagnetic interference/compatibility (EMI/EMC) communities, and government/contractor laboratories. The U.S. concentrates on lethality assessment; the effects program is spread between the services, and there is little involvement of the EMI/EMC community.

3.2.9 Conclusion

If readers gather from this survey that HPM weapons face a complex set of factors that influence their true military utility, they are correct. The complexity of HPM DEWs requires a systematic approach with careful consideration of utility as a weapon, meaning an engagement analysis, coupling analysis and testing, electronic component testing, system testing, and a countermeasure (hardening) study.

As in the episode at the beginning of this section, easy, speedy battlefield use is critical. Only systematic integration with existing network-centric systems can give the warfighter quick, useful weapons. Just as "fire and forget" became a paradigm, so could "HPM kill."

3.3 High Power Radar

Radar applications for HPM depend not on the higher power directly, but rather on very short pulses at high repetition rate at high power. Here we cover short pulses (<10 nsec) at high power: ultrashort pulse radar, called ultrawideband (UWB) radar.

The most obvious application of HPM to radar is simply to increase the transmitter power P_T, thus increasing the maximum detection range for a target with a specified radar cross section. In radar, all other things being fixed, the maximum detection range scales as $P_T^{1/4}$; therefore, increasing a high power radar from 1 MW to 10 GW will increase the detection range by an order of magnitude. However, for conventional radar the limitation is not power, but signal-to-noise ratio produced by ground clutter and other interfering effects. Therefore, simple power scaling does not address the real limitations of conventional radar. The most fruitful use of HPM in radar is to address some of conventional radar's basic limitations.[13]

A basic issue is *dead time*, the time when the receiver is turned off while the transmitter operates. Using shorter pulses minimizes this, but the radar must also have a good return signal at the desired range. The solution is to operate at GW power levels with pulses just long enough to have a bandwidth about that of a wideband receiver. A shorter pulse would give a reduced receiver signal due to some of the power being out of band.

The most developed HPM radar is the[14] NAGIRA system (Nanosecond Gigahertz Radar) built in Russia and comprehensively tested in the U.K. The system, shown in Figure 2.15 and Figure 2.16, is based on a SINUS-6, in which a Tesla transformer charges a coaxial oil-filled pulse-forming line (PFL) to 660 kV. The line is discharged by a triggered gas switch into a transmission line that tapers to 120 Ω impedance at 660 kV to match that of a backward wave oscillator. This produces 7-nsec pulses and operates up to 150 Hz in X-band (10 GHz, so 70 cycles and ~2% bandwidth). After TE_{01}-to-TM_{11} mode conversion, the extracting waveguide terminates at a feed horn with a vacuum window through which the Gaussian-shaped excitation illuminates an offset, 1.2-m parabolic reflector antenna, forming a pencil beam with a beam width of 3° (see Problem 5).

Range resolution of a radar is given by $\delta = c\tau/2$, where τ is the duration of the pulse, so that a 10-nsec radar signal will give a range resolution of about 1.5 m. Each radar range cell in the signal processor is only 1 m long. Therefore, large extended targets can have their "portraits painted" by a series of signals coming from different parts of the target.[15] This allows some degree of target identification in principle, and experiments show that it works in practice. NAGIRA can detect a small airplane at 100 km. Range resolution is ~1 m, so targets can be identified.

An important factor is pulse-to-pulse frequency stability because the moving target motion is detected by separating from clutter by subtracting subsequent pulses. Therefore, voltage and current into the BWO must be controlled. Using short high power pulses makes possible precise range resolution for detection and tracking of low-cross-section moving targets in the presence of strong local reflections.

Gyrotrons and relativistic magnetrons would also be good choices for this radar because they too can produce high power at higher frequencies. Outstanding technical issues for HPM radar remain. Principal among them are cathode life and scanning antennas at high power. The cathode life of the NAGIRA graphite cathodes, as well as other explosive emission materials, is 10^8 shots; a much longer lifetime would be needed in a practical device. To enable scanning of the beam on azimuth and elevation will require a high power rotating joint in the antenna feed.

3.4 Power Beaming

A variety of schemes have been suggested for transferring energy from Earth to space, space to Earth, space to space, and between points on Earth using HPM beams. The purpose is to beam large amounts of energy; the peak and average power requirement is set by the duration of the application.[16] Some of the applications are solar-powered satellite-to-ground transmission, intersatellite power transmission, and short-range applications such as between parts of a large satellite or from a lander to a rover in interplanetary exploration.[17] Another class of applications of directed power beams where the receiving area is a target includes microwave weapons and ionosphere modification by artificial ionization of the upper atmosphere for radar or atmospheric chemistry.[18] Free-space transmission is desirable because it is far more efficient over long distances (>100 km) than competitor techniques, such as coax cable, circular waveguide, or fiber-optic cable.[19]

All such applications depend on far-field transfer, where the separation between transmitting antenna and receiving area is greater than or equal to the far-field distance $2D^2/\lambda$, where D is the diameter of the largest area and λ is the wavelength. (However, the method described here can also be applied in the near field with a focused transmit antenna. This is best done with a phased-array antenna to produce a focused pattern with spot size less than D_t.) The electromagnetics are quite general, depending on only the basic parameters of the system.

The schematic is shown in Figure 3.16. The transmitting antenna of area A_t places its beam on the receiving area A_r, which can be another antenna, a rectenna, or a target, such as a spacecraft. At the range R, the beam, defined by its half-power beam width, will typically be larger than A_r.

In an exact general treatment,[20] the power transfer efficiency for circular apertures is governed by the power–link parameter

$$Z = \frac{D_t D_r}{\lambda R} \tag{3.7}$$

where D_t and D_r are the diameters of the transmitting and receiving antennas, respectively, and R the distance between transmitter and receiver. For efficient transfer, the spot size must be ~D_r and $Z \geq 1$.

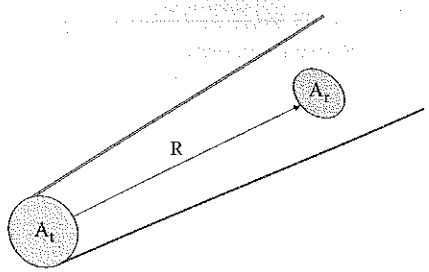

FIGURE 3.16
Power beaming schematic; transmitting and receiving areas separated by distance R.

To understand the power–link relation, note that the power received on a target is the power density integrated over the target area. If the transmitting antenna has an isotropic radiation pattern, then the power density S is just the power P distributed over the surface area of a sphere through which the power passes:

$$S = \frac{P}{4\pi R^2} \tag{3.8}$$

The typical case is that the beam is focused by the antenna (see Chapter 5). If it has a gain G, then the power density is enhanced to

$$S = \frac{PG}{4\pi R^2} \tag{3.9}$$

The antenna gain is

$$G = \frac{4\pi\varepsilon A_t}{\lambda^2} \tag{3.10}$$

where ε is the antenna efficiency, also called the aperture efficiency, and A_t is the transmitting antenna area. The efficiency with which power is received is then roughly

$$\frac{P_r}{P_t} = \left(\frac{\pi}{4}\right)^2 \varepsilon \left[\frac{D_t D_r}{\lambda R}\right]^2 = \left(\frac{\pi}{4}\right)^2 \varepsilon Z^2 \tag{3.11}$$

The efficiency of transfer varies roughly with the square of Z. This is approximate because this simple analysis does not average over the target area or take into account the antenna pattern and is invalid above Z ~ 1.

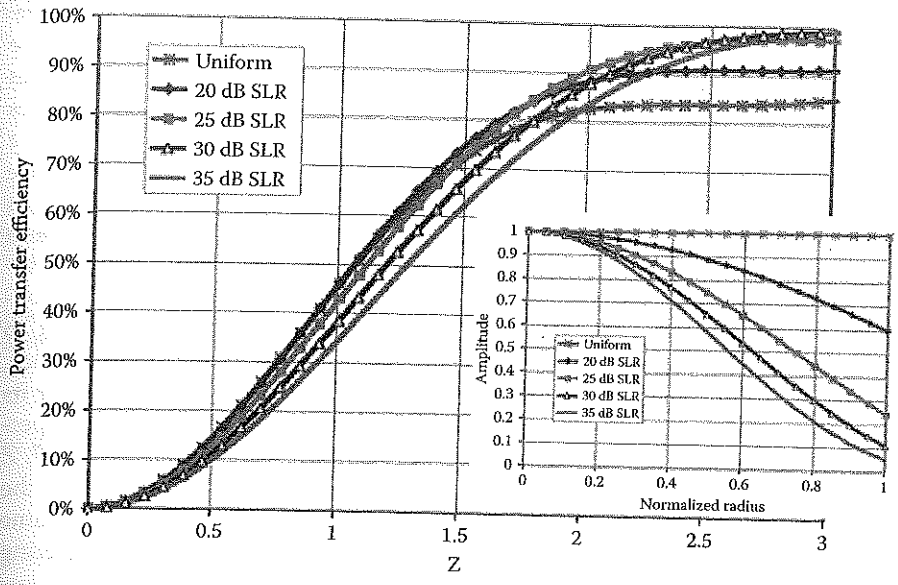

FIGURE 3.17
Power transfer between distant apertures as a function of principal parameters, $Z = D_t D_r/\lambda R$. Controlling sidelobe ratio (SLR) by tapering the power across the antenna (inset, see Ref. 20) reduces side radiation but broadens beam width.

An exact treatment gives the curve of Figure 3.17. Power transfer can be made efficient by proper choice of diameters and wavelength for a specific range. Choosing Z = 2 gives high efficiency, but Z = 1.5 may well be a more practical compromise to reduce aperture areas. An approximate analytic expression, suitable as a rule of thumb, for the exact solution in Figure 3.17 is

$$\frac{P_r}{P_t} = 1 - e^{-Z^2} \tag{3.12}$$

For comparison, for Z = 1, and uniform aperture amplitude distribution, Equations 3.11 and 3.12 give 62% efficiency and the exact solution gives 48%.

These efficiencies are for circular polarization-matched antennas; linear or dual-linear polarization can lead to additional losses. They also do not include losses due to propagation effects and intervening attenuations, such as that from atmosphere.

Note in the inset in Figure 3.17 that the transmitting antenna *taper*, defined as gradual reduction of amplitude toward the edge of the transmitting antenna of the array, has a great influence on efficiency. The abruptness with which the amplitude ends at the edge of the antenna is closely related to how much energy is found in sidelobes. In many cases, the power transfer

efficiency is regulated by the desired sidelobe ratio (SLR), to avoid interference with other platforms, for example. A 25-dB SLR means the first sidelobe is 25 dB down (reduction factor of 316) from the main beam, and it requires that a specific amplitude taper be applied to the aperture. Higher SLR values reduce the amount of power radiated in the sidelobes at the expense of a broader beam width. A 25-dB SLR taper provides a good compromise between low sidelobes and high power transfer efficiency.

The power beaming relation scaling shown in Figure 3.17 has been demonstrated many times and is well documented.[2] Efficiencies of aperture-to-aperture transfer from transmitter to receiver of >80% have been demonstrated, although designs typically compromise efficiency somewhat to improve other factors, such as cost and ease of assembly and maintenance. As an example, consider an aircraft at 1-km altitude receiving power for its propulsion from an antenna radiating at 12 GHz from a 4-m-diameter aperture. If the receiving rectenna has a diameter of 12.9 m, from Figure 3.17, Z = 1.98 and collection efficiency is 90%. However, if the rectenna on the aircraft were elliptical, perhaps to provide conformal fit, but with the same area as the circular rectenna, the efficiency would be reduced by the differing power distributions.

The diffraction-limited beam width is

$$\theta = 2.44\ \lambda/D_t \tag{3.13}$$

This is the diffraction-limited divergence, giving the first null point of the Bessel function for a circular aperture and including 84% of the beam power. The spot size is just $D_s = \theta\ R = 2.44\ \lambda\ R/D_t$. For example, a 2-m-diameter ground-based transmitter at 35 GHz radiates to an aircraft 1 km away. For a 7.5-m receiving aperture (or target size), Z = 1.75 and 83% of the beam is received. The beam width is 0.6° and spot size is 10.5 m.

At the receiving end, the *rectenna*, a rectifying antenna, a component unique to power beaming systems, converts microwave power to DC power. It consists of an array of antenna elements, usually simple dipoles, each terminated with a rectifying diode. The circuit elements are shown in Figure 3.18 and many are shown in Figure 3.19. Diodes rectify most efficiently when the DC output voltage is operating at half the diode's breakdown voltage. Efficiency varies with power density on the element; most work to date has been at densities on the rectenna of 10 to 100 mW/cm^2. Because a rectenna element is terminated by a diode and RF shorting filter, the array radiation pattern resembles the cosine pattern of a single dipole element. No sidelobes are created by the rectenna array (see Problem 6). But there can be radiation of self-generated harmonics due to circuit nonlinearities. High rectenna efficiencies can be achieved, but only with proper selection of diode parameters. The chief limiting factor is high cutoff frequency, meaning that frequency is constrained by achieving low-diode junction capacitance and low series resistance.

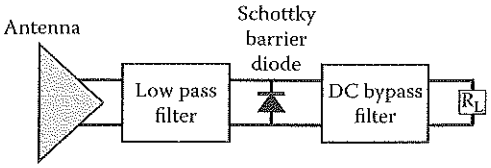

FIGURE 3.18
Rectenna converts microwaves to DC electrical energy. The antenna is typically a horizontal dipole placed 0.2λ above a reflecting ground plane. Filters contain the self-generated harmonics produced by the diode and provide the proper impedance match to the diode at the power beaming frequency. (Reprinted from McSpadden, J.O. and Mankins, J.C., *IEEE Microwave Mag.*, 3, 46–57, 2002. By permission of IEEE.)

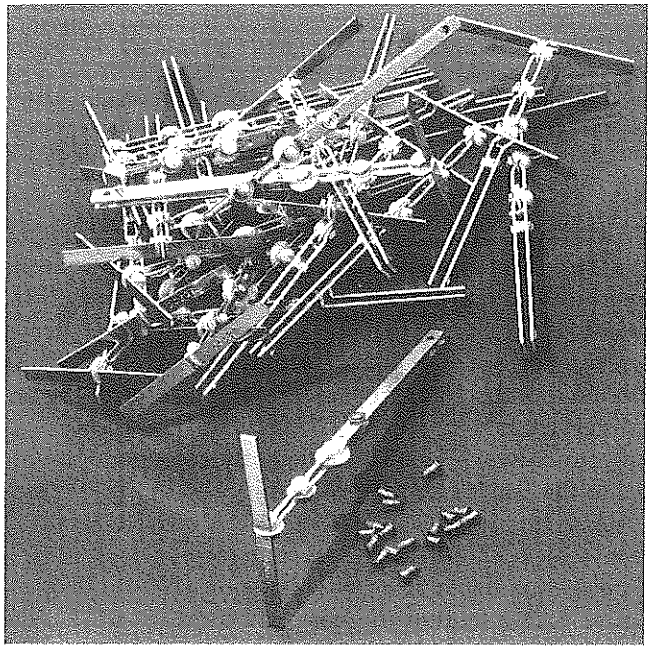

FIGURE 3.19
Group of typical rectenna elements, dipoles, diodes, and circuitry. (Reprinted from McSpadden, J.O. and Mankins, J.C., *IEEE Microwave Mag.*, 3, 46–57, 2002. By permission of IEEE.)

Rectenna experiments have demonstrated up to 54% DC-to-DC power transfer efficiency at 2.45 GHz, and there is some work on higher frequency rectennas.[21] Figure 3.20 shows the highest recorded rectenna efficiencies at 2.45, 5.8, and 35 GHz. Aircraft and blimps have been flown, sometimes for considerable times, on power beams.[22,23] A demonstration of power beaming over a 1.5-km distance produced a received power of 34 kW at 2.388 GHz by Dickinson[24] and Brown.[25]

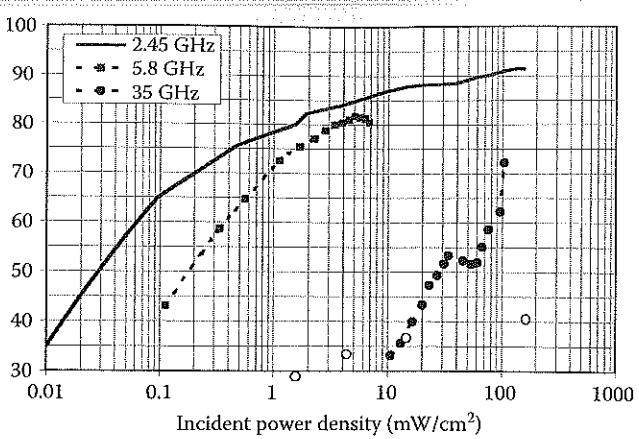

FIGURE 3.20
Highest measured rectenna conversion efficiencies. The numbers on the 2.45-GHz curve indicate the efficiency using GaAs/W Schottky diodes with varying breakdown voltages. (Reprinted from McSpadden, J.O. and Mankins, J.C., *IEEE Microwave Mag.*, 3, 46–57, 2002. By permission of IEEE.)

William Brown, who invented the rectenna, conducted detailed development for space applications of it, most especially an interorbital ferry for transporting from low Earth orbit to geosynchronous orbit.[25] It would use beamed power to a large array (225 m²) of rectennas, which drive ion thrusters continuously. For a cargo mass fraction of ~50%, orbit-raising transit times are about 6 months. Power beamed to the ferry is of the order 10 MW, with a low duty factor.

The use of a microwave beam to efficiently transport power from solar cells in space to the Earth's surface was proposed in the 1960s and reinvestigated by NASA in the 1990s.[26] The reference system concept, a large capital-intensive no-pollution energy system for the 21st century, is ~10 GW continuous power available at an efficiency of >50%. As shown in Figure 3.21 and Figure 3.22, a station in geosynchronous orbit (22,300 miles altitude) emits a narrow beam (0.3 mrad) at frequencies in S-band (2.45 GHz). Basic issues are efficient conversion of the DC power to microwave power and preeminently the construction of extremely large massive antennas (apertures in space typically 1 km across and a rectenna array about 7 km on the Earth).[27]

The microwave tube requirement could be met by a vast distributed array of crossed-field amplifiers, magnetrons, gyrotrons, or klystrons operating at average powers of ~10 kW each. Magnetrons for continuous operation are now available at 100 kW. Therefore, ~10^5 tubes would be required and low-cost production techniques would need to be developed to keep the cost practical. Higher-average-power MW-class gyrotrons (Chapter 10) could be competitive, but they operate at higher frequencies. For example, commercially available continuous-wave (CW) gyrotrons are capable of

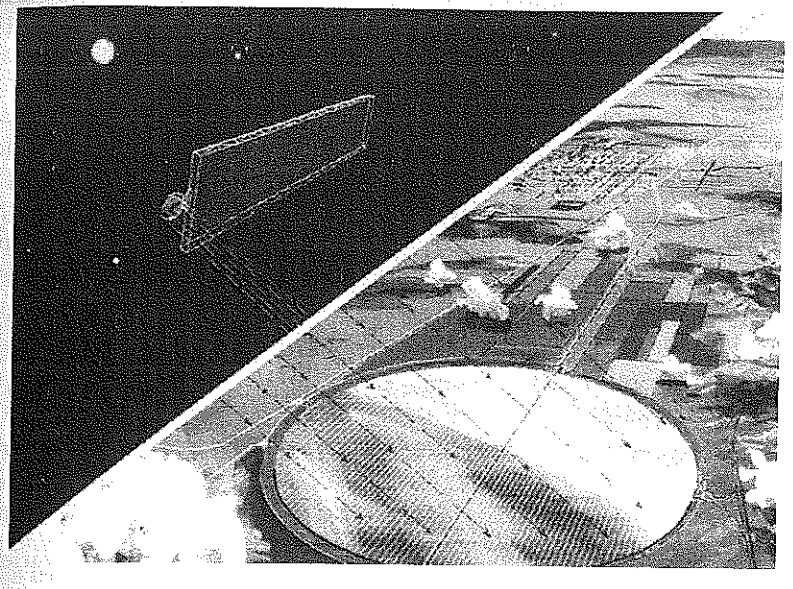

FIGURE 3.21
Solar power satellite beams enormous microwave power to rectenna farm for distribution.

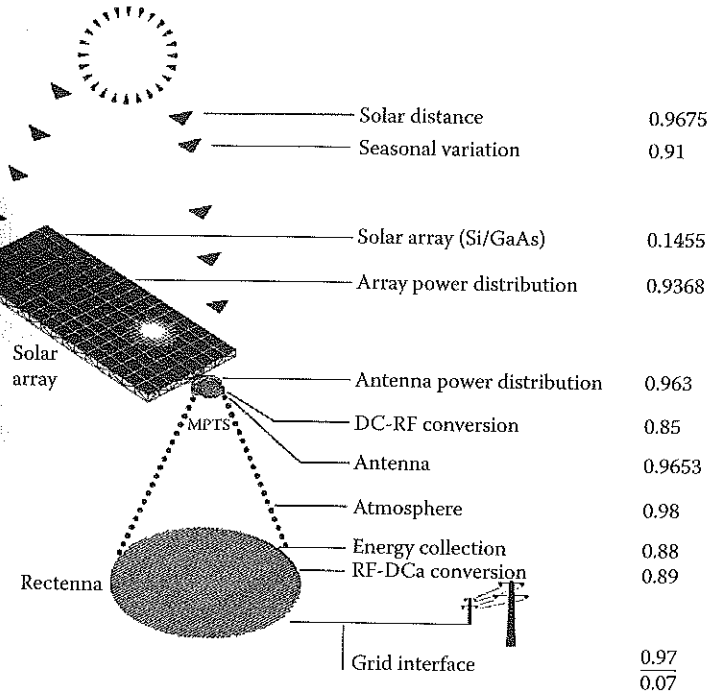

FIGURE 3.22
Solar power satellite estimated efficiencies.

MW-class powers in the 35- and 94-GHz atmospheric window (see Chapters 5 and 10). An alternative is a much larger number of solid-state sources at much lower power.

The basic issue for all space-to-Earth power transmission schemes is not technical, but economic. The costs are strongly contested[28] and will determine the practicality of large-scale CW HPM systems in space. It is at best a distant prospect. An even larger-scale proposal is to deliver energy from solar power stations on the moon built from all lunar materials, beaming power directly to receiving sites on Earth.[29] A reciprocal application wherein the power is beamed upward from Earth to low Earth orbit satellites requires ~10- to 100-MW power levels for tens of seconds.[30]

3.5 Space Propulsion

Microwave beams have been studied for moving spacecraft by a variety of means:

- Launch to orbit
- Launch from orbit into interplanetary and interstellar space
- Deployment of large space structures

3.5.1 Launch to Orbit

Today, payloads are launched into orbit the same way they were 50 years ago — by chemical rockets. Expendable multistage rockets usually achieve payload fractions of less than 5%. As described by the rocket equation, this is due partly to the structural limits of existing materials and partly to the limited efficiency of chemical propellants. The rocket equation, which drives the advance of space exploration, is simply derived.[31] If a rocket of mass M produces momentum change by expelling a small amount of reaction mass dM at high velocity V_e, the change in rocket velocity is, from momentum conservation,

$$MdV - V_e dM \tag{3.14}$$

By integration, when the fuel is spent so that the initial mass M_o is reduced to a final mass M_f, the resulting change in rocket velocity,

$$\Delta V = V_e \ln M_o/M_f \tag{3.15}$$

Since the natural logarithm increases very slowly with the mass ratio, large mass ratios do not produce large ΔV. Another way to see this is

$$\frac{M_o}{M_f} = e^{\frac{\Delta V}{V_e}} \tag{3.16}$$

which means that getting the high velocities needed for orbit or interplanetary probes with a single rocket is almost impossible because the rocket structural mass is too high relative to the fuel mass (see Problem 7). The structural economies made to preserve these minute payload fractions result in fragile, expensive-to-build rockets. Despite 50 years of incremental rocket development, better materials, novel propellants, and modestly improved reliability have left the basic economics of launch unchanged at a payload cost of around $5000/kg of delivered payload.[32] This makes space development and exploration very expensive. If price can be lowered, an increase in demand great enough to offset lower prices and increase the overall market size is thought to exist only at a price point below $1000/kg. It is doubtful that conventional chemical rocket launches will ever be able to reach such a price.

This led Parkin[33] to propose new HPM-based launch schemes, which offer greater I_{sp} than possible with conventional systems. (The efficiency of a rocket, how many seconds a pound of fuel can produce a pound of thrust, is termed specific impulse, I_{sp}. Chemical rockets have reached a practical limit of $I_{sp} < 500$ sec.)

The physics of HPM propulsion are different, and in some ways more complex, than conventional propulsion. The microwave thermal rocket, shown in Figure 3.23, is a reusable single-stage vehicle that can afford the mass penalty of robust, low-cost construction because it a uses a high-performance microwave thermal propulsion system with double the I_{sp} of conventional rockets.[34,35] It is premature to quantify the reduction in transportation costs that these simplifications will bring, but clearly the cost reduction could be dramatic, transforming the economics of launch to space.

Microwave thermal thrusters operate on an analogous principle to nuclear thermal thrusters, which have experimentally demonstrated specific impulses exceeding 850 sec. (The large weight of the nuclear reactors relative to the thrust the propulsion systems produce precludes their use in practical rockets.) It is a reusable single-stage vehicle that uses a HPM beam to provide power to a heat exchanger-type propulsion system, called the *microwave thermal thruster*. By using HPM, the energy source and all the complexity that it entails are moved onto the ground, and a wireless power transmission system is used between the two. When Parkin and Culick proposed this system[36] and analyzed its performance, they found that beam divergence and aperture area are key constraints for such a system and devised a high-acceleration ascent trajectory, which provides most of the transfer of energy at short range, in order to minimize the size of the radiating aperture required. For such a system, the power–aperture–efficiency trade given in Equation 3.17 is key to minimizing the cost, which could potentially fall to

FIGURE 3.23
Microwave thermal rocket in flight. (Reprinted by permission of Dr. Kevin Parkin.)

as low as a few times the *energy* cost of launch (as opposed to capital cost of the system), which is around $50/kg for such a system.

Ascent trajectory analysis predicts a 10% payload fraction for a 1-ton payload on a single stage to orbit a microwave thermal rocket. By using a single reusable stage with high specific impulse, low-cost and reusable launchers are possible. For comparison, the Saturn V had three nonreusable stages and achieved a payload fraction of 4%. In Figure 3.24, the spacecraft flat aeroshell underside is covered by a thin microwave absorbent heat exchanger that forms part of the thruster. The exchanger is likely to be of silicon carbide and consists of ~1000 small channels carrying fuel to the motor. The rocket can be launched by a conventional first stage, by airdrop into the vicinity of the beam, or by a physically small but powerful microwave source located at the launch site, which powers the first few kilometers of atmospheric ascent before it is acquired by the main beam.

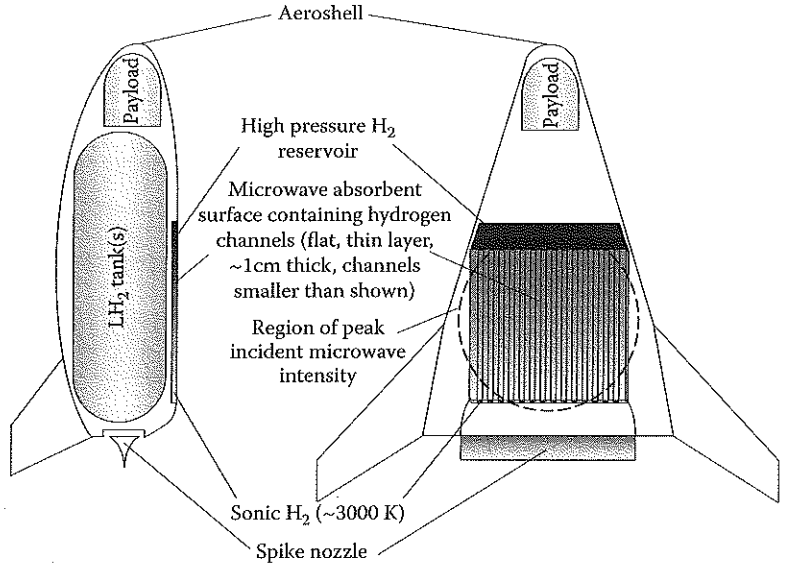

FIGURE 3.24
Major elements of the microwave thermal rocket. Vehicle length is 6 m, 5 m width at base. Payload is 100 kg; structure, 180 kg; LH_2 fuel, 720 kg. (Reprinted by permission of Dr. Kevin Parkin.)

During the ~3-min powered ascent, acceleration varies from 2 to 20 g, so as to stay in range of the beam source. The vehicle length is 6 m, 5 m wide at base. During ascent, the heat exchanger faces the microwave beam. Using a phased-array source, a high-intensity 3-m-diameter microwave spot can be projected onto the underside of a launcher over 100 km away.

The power density of 300 MW impinging on a 7-m^2 converter on the underside drives the hydrogen fuel to temperatures of 2400 K. Microwave frequency determines the maximum beam energy density via the constraint of atmospheric breakdown. Ionizing air into plasma can distort and reflect the incoming beam (see Chapter 5). Atmospheric breakdown occurs more easily at low frequencies, because fields have more time to accelerate background electrons. The continuous-wave (CW) atmospheric breakdown intensity, shown in Figure 3.25, demonstrates that a 300-GHz beam can achieve 1000 times the power density of a 3-GHz beam. A microwave beam of 300 MW on a 3-m spot means that the power density will average ~40 MW/m^2, so frequencies above ~25 GHz are needed to prevent breakdown. High-frequency operation above ~100 GHz is preferable because the array area needed decreases substantially as beam frequency increases.

The feasibility and design of a 30-MW, 245-GHz, ground-based beam launcher facility using an array of parabolic dishes were described in papers by Benford, Myrabo, and Dickinson[37,38] in the 1990s. The average power output of gyrotron sources used has significantly increased to commercially available 1-MW gyrotron sources operating at ~100 GHz. Three hundred

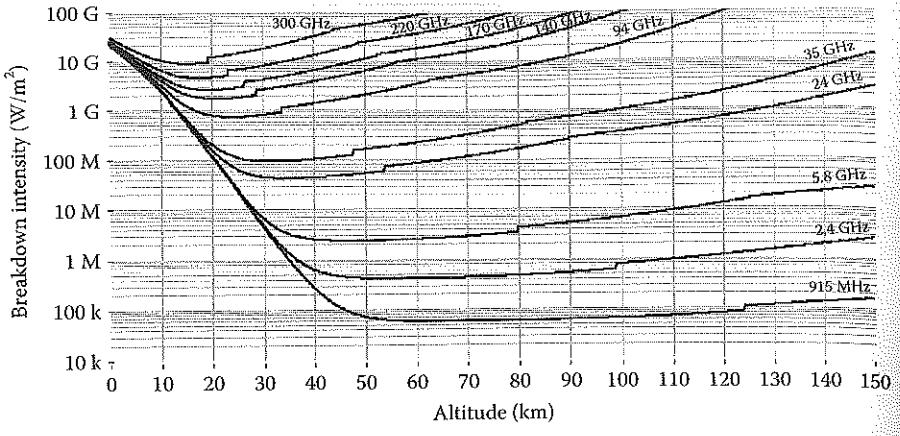

FIGURE 3.25
Breakdown variation with altitude and frequency. Launch to orbit requires higher frequencies. (Reprinted by permission of Dr. Kevin Parkin.)

such sources would be sufficient to propel a 1-ton craft into Low Earth Orbit (LEO). The gyrotron can be either an amplifier or a phase-injection-locked oscillator.[39] In the former unit, the array beam steering is done simply by a combination of mechanical pointing and phase shifting the module drive signal. In the latter case, the beam steering is done by a combination of mechanical pointing and phase shifting, but must also include means such as a magnetic field strength trim to set the rest frequency of the oscillator (Chapter 10).

Figure 3.26 gives the layout of a 245-GHz, 30-MW ground-based power beaming station.[38] It has a span of 550 m and contains 3000 gyrotrons at 10 kW of power. A single radiating element is the 9-m dish shown in Figure 3.27.

Augmentation of rocket engines for launch to orbit have also been suggested by beaming to rectennas.[40] A crucial limitation of such schemes is the weight of the rectenna, 1 to 4 W/g, which needs improvement of an order of magnitude for space applications. Supporting a platform in the upper atmosphere at ~70 km by means of the radiometric effect using a ~1-MW microwave beam to heat the underside of the vehicle has also been analyzed and seems practical.[41]

The cost of such large HPM systems described here is driven by two elements: the *capital cost*, including the cost of the microwave source and the cost of the radiating aperture, and the *operating cost*, the cost of the electricity to drive the system:

$$C = C_C + C_O$$
$$C_C = C_S + C_A \qquad (3.17)$$
$$C_O = C_E$$

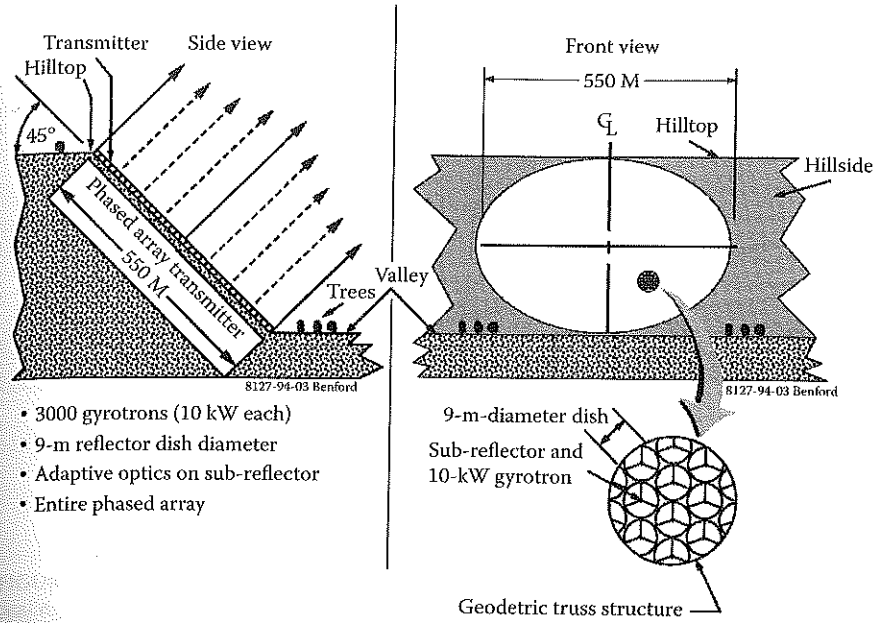

FIGURE 3.26
Ground-based power beaming station.

A simple approach is to assume linear scaling with coefficients describing the dependence of cost on area $B_1(\$/m^2)$, microwave power $B_2(\$/W)$, and prime power $B_3(\$/W)$:

$$C_A = B_1 D_t^2 \frac{\pi}{4}$$
$$C_S = B_2 P$$
$$C_E = B_3 P \qquad (3.18)$$
$$C_C = B_2 P + B_1 D_t^2 \frac{\pi}{4} + B_3 P$$

An empirical observation made independently by Dickinson[38] and O'Loughlin is that, for a fixed effective isotropic radiated power (EIRP; the product of radiated power and aperture gain), *minimum capital cost is achieved when the cost is equally divided between antenna gain and radiated power.* Here, the gain includes the antenna, its supports, and subsystems for pointing and tracking. Power cost includes the source, power supply, and cooling equipment. If this rule of thumb holds,

$$C_S = C_A,\ C = [2B_2 + B_3]P \qquad (3.19)$$

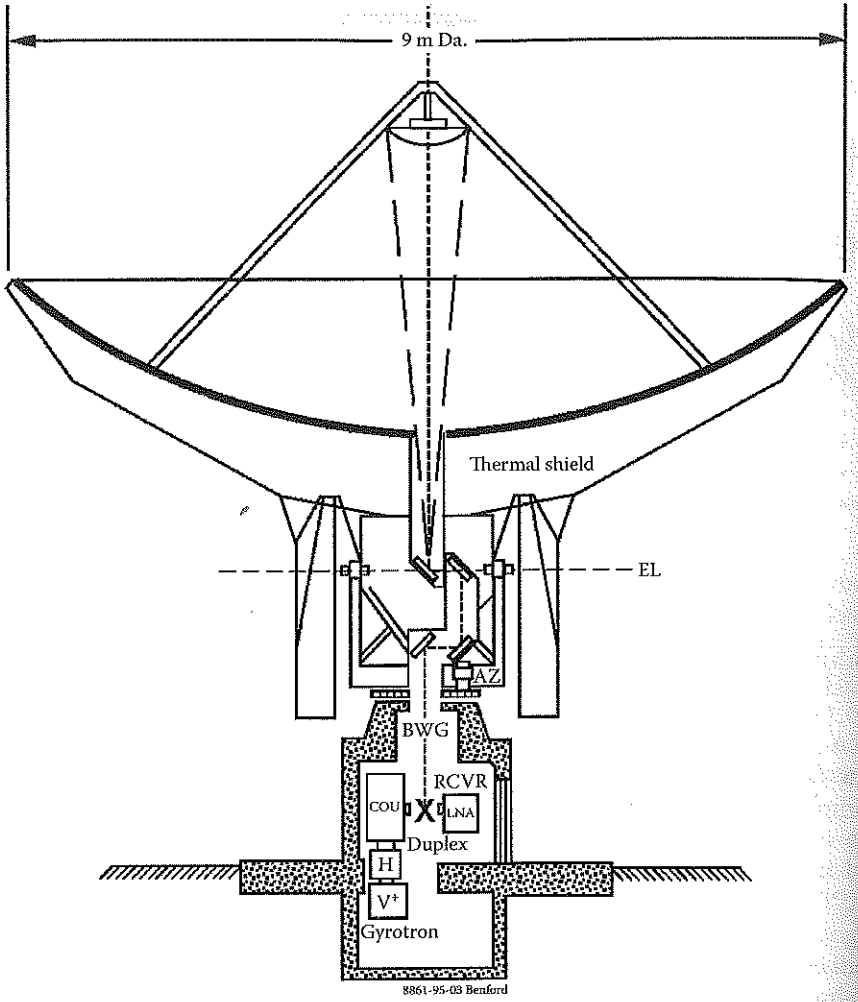

FIGURE 3.27
Single 9-m dish element for the ground-based power beaming station. Beam Waveguide (BWG) feeds dish from gyrotron, reflected signal received (RCVR) by low noise amplifier (LNA).

Only rough estimates of the capital costs are possible with such a simple model. However, when mission specifics are introduced, giving additional constraints, useful scalings result. Kare and Parkin have cost modeled a microwave thermal rocket.[42] They also account for the *learning curve*, the decrease in unit cost of hardware with increasing production. This is expressed as a learning curve factor f, the cost reduction for each doubling of the number of units. The cost of N units is

$$C_N = C_1 N^x \tag{3.20}$$

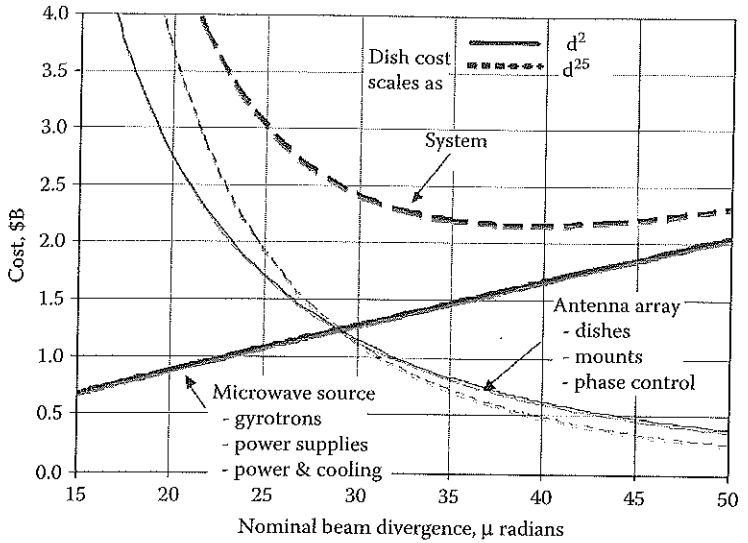

FIGURE 3.28
Scaling of aperture and source cost (including prime power) for the microwave launcher system as a function of the beam divergence.

For cost scaling, exponent $x = 1 + \ln(1 - f)/\ln 2$, e.g., a 15% learning curve corresponds to an exponent of 0.76. For example, if gyrotron cost scales as the power P, but if there is a 15% learning curve, cost scales as $P^{0.76}$. MW units costing \$1/W in single units will cost \$0.28/W for 200 units.

For antenna costs, data exist that scale cost with diameter D^{δ} to an exponent ranging from $\delta = 2$ to 2.5. Figure 3.28 shows the scaling of the aperture cost and source cost (including prime power) for the microwave system as a function of the beam divergence, for $\delta = 2.0$ and 2.5. (Both the number and size of the antennas enter into the calculation, so the total array cost varies as $D_t^{\delta-2x}$.) Note that the Dickinson observation holds approximately: the cost minimum is close to where the source and antenna costs are equal.

3.5.2 Launch from Orbit into Interplanetary and Interstellar Space

Microwave-propelled sails are a new class of spacecraft that promises to revolutionize future space travel. For a general introduction to solar and beam-propelled sails, refer to McInnes.[43]

The microwave-driven sail spacecraft was first proposed by Robert Forward as an extension of his laser-driven sail concept.[44] The acceleration from *photon momentum* produced by a power P on a thin sail of mass m and area A is

$$a = [\eta + 1]P/m\,c \tag{3.21}$$

where η is the reflectivity of the film of absorbtivity α and c is the speed of light. The force from photon acceleration is weak, but is observed in the trajectory changes in interplanetary spacecraft, because the solar photons act on the craft for years. For solar photons, with a power density of ~1 kW/m^2 at Earth's orbit, current solar sail construction gives very low accelerations of ~1 mm/sec^2. Shortening mission time means using much higher power densities. In this case, to accelerate at one Earth gravity requires ~10 MW/m^2 (see Problems 8 and 9).

Of the power incident on the sail, a fraction αP will be absorbed. In steady state, this must be radiated away from both sides of the film, with an average temperature T, by the Stefan–Boltzmann law:

$$\alpha P = 2A\,\varepsilon\,\sigma\,T^4 \tag{3.22}$$

where σ is the Stefan–Boltzmann constant and ε is emissivity. Eliminating P and A, the sail acceleration is

$$a = 2\,\sigma/c[\varepsilon\,(\eta + 1)/\alpha](T^4/m) = 2.27 \times 10^{-15}\,[\varepsilon(\eta + 1)/\alpha](T^4/m) \tag{3.23}$$

where we have grouped constants and material radiative properties separately. Clearly, the acceleration is strongly temperature limited. This fact means that materials with low melt temperatures (Al, Be, Nb, etc.) cannot be used for fast beam-driven missions. Aluminum has a limiting acceleration of 0.36 m/sec^2. The invention of strong and light carbon mesh materials has made laboratory sail flight possible[45] because carbon has no liquid phase and sublimes instead of melting. Carbon can operate at very high temperature, up to 3000°C, and limiting acceleration is in the range of 10 to 100 m/sec^2, sufficient to launch in vacuum (to avoid burning) in Earth-bound laboratories.

Recently, beam-driven sail flights have demonstrated the basic features of the beam-driven propulsion. This work was enabled by invention of strong, light carbon material, which operates at high enough temperatures to allow liftoff under one Earth gravity. Experiments with carbon–carbon microtruss material driven by microwave and laser beams have observed flight of ultralight sails at several gee acceleration.[46] In the microwave experiments, propulsion was from a 10-kW, 7-GHz beam onto sails of mass density of 5 g/m^2 in 10^{-6} Torr vacuum. At microwave power densities of ~kW/cm^2, accelerations of several gravities were observed (Figure 3.29). Sails so accelerated reached >2000 K from microwave absorption and remained intact. Photonic pressure accounts for up to 30% of the observed acceleration. The most plausible explanation for the remainder is desorption pressure and evaporation of absorbed molecules (CO_2, hydrocarbons, and hydrogen) that are very difficult to entirely remove by preheating. The implication is that this effect will always occur in real sails, even solar sails at low temperature, and can be used to achieve far higher accelerations in the initial phase of future sail missions.

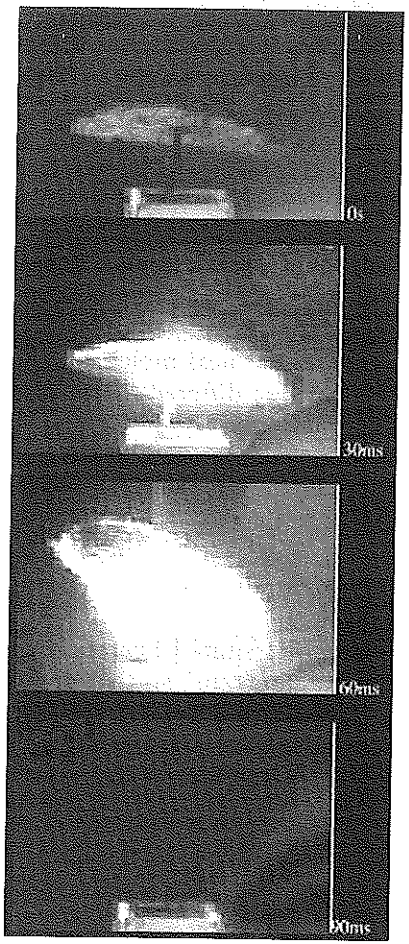

FIGURE 3.29
Carbon sail lifting off of a rectangular waveguide under 10 kW of microwave power (four frames, first at top). Frame interval is 30 msec.

This other acceleration mechanism, *desorption pressure*, is due to mass ejected from the material downward to force the sail upward:

$$F = v_T\,dm/dt \tag{3.24}$$

where v_T is the thermal speed of the evaporated material — carbon or molecules absorbed into the carbon substrate. The magnitude of this effect can vastly exceed the microwave photon pressure if the temperature is high enough because it couples the energy of photons, not the momentum, as in photon pressure. The essential factor is that this force must be asymmetric; if the sail is isothermal, there is no net thrust. Thermal analysis shows that, although for thin material thermal conduction reduces such differences

greatly, the skin effect produces a substantial temperature difference between the front and back of sails.

A variety of compounds not typically thought of as fuels can be "painted" on sails and, depending on which physical process occurs, sublimed, evaporated, or desorbed. Atoms embedded in a substrate can be liberated by heating, an effect long studied in the pursuit of ultraclean laboratory experiments. This effect is called *thermal desorption* and dominates all other processes for mass loss above temperatures of 300 to 500°C.

A molecule is *physisorbed* when it is *adsorbed* without undergoing significant change in electronic structure, and *chemisorbed* when it does. Physisorbed binding energies (~2 to 10 kcal/mole) are typically much less than chemisorbed energies (~15 to 100 kcal mole), by as much as an order of magnitude. This implies that two different regimes of mass liberation can be used, with physisorbed molecules coming off at lower temperatures, and hence lower thrust per mass, while chemisorbed molecules can provide higher thrust per mass. Cuneo[47] offers this general schematic for desorption in layers from bulk substrates: the rate of mass loss under heating is

$$dn/dt = an\ e^{-Q/kT} \tag{3.25}$$

where a is $\sim 10^{13}$ sec^{-1}, Q is the required liberation energy (usually <1 eV), and n is the area density in atoms/m^2, so that dn/dt is the desorbed flux under heating in atoms/m^2-sec. (We neglect readsorption, which is tiny in a space environment.) The exponential factor means that thermal desorption of molecules from a sail lattice will have a sudden onset as the sail warms. When temperature T varies with time, the equation can be formally solved:

$$n(t)/n^\circ = \exp\{-a \exp[-Q/kT(t)]\ dt\} \tag{3.26}$$

As the binding energy Q increases, the time to desorb gets longer. The relationship between Q and T*, the temperature at the peak in the desorption rate dn/dt, is, for heating rate dT/dt,

$$Q/kT^{*2} = a \exp(-Q/kT^*)/(dT/dt) \tag{3.27}$$

At the peak desorption rate, 63% of the mass inventory has been lost, so this is a good estimate of when the effect is largest for a given molecule of binding energy Q.

Hydrogen is often easiest to liberate, with a Q of 0.43 to 1.5 eV, depending on the substrate. Water has Q = 0.61 eV. Generally, candidate chemisorbed compounds like hydrocarbons have a Q of around 1 eV (11,605 K). CO is more strongly bound and may be the most tightly held in a carbon sail lattice. Sails experiencing strong, sudden-onset lift may be desorbing CO at a critical temperature onset of >2300 K (see Problem 10).

An early mission for microwave space propulsion is dramatically shortening the time needed for solar sails to escape earth orbit. By sunlight alone,

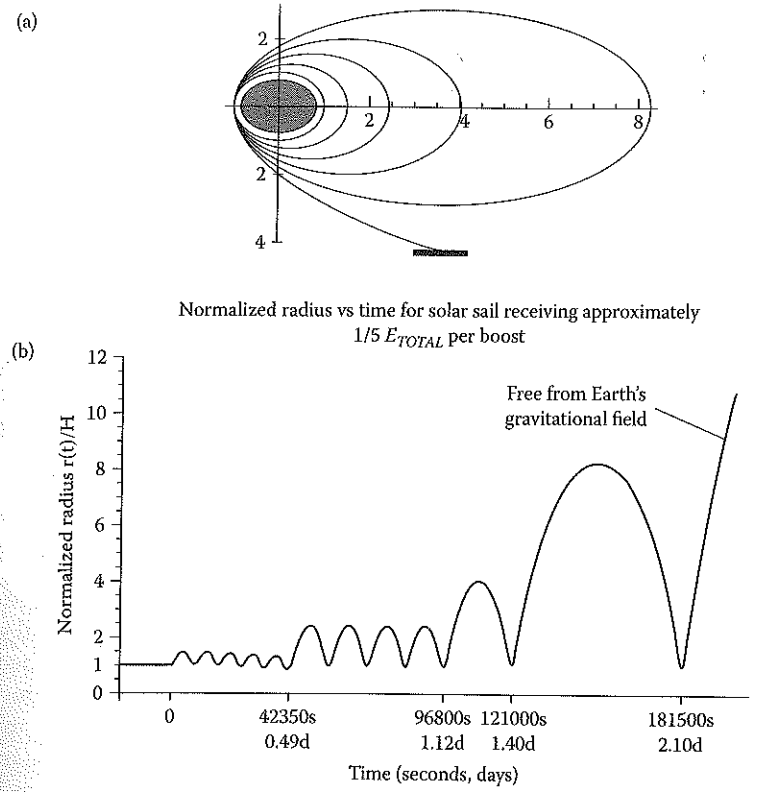

FIGURE 3.30
(a) Beam-driven sail trajectory out of Earth orbit. Units are the radius normalized to the initial height H. Solar sail is not to scale. (b) Radius normalized to Earth radius vs. time for solar sail. (Reprinted by permission of Dr. Gregory Benford, University of California–Irvine.)

sails take about a year to climb out of the Earth's gravity well. Computations show that a ground-based or orbiting transmitter can impart energy to a sail if it has resonant paths — that is, the beamer and sail come near each other (with either the sail overhead an Earth-based transmitter or the sail nearby orbits in space) after a certain number of orbital periods. For resonance to occur relatively quickly, specific energies must be given to the sail at each boost. If the sail is coated with a substance that sublimes under irradiation, much higher momentum transfers are possible, leading to further reductions in sail escape time. Simulations of sail trajectories and escape time are shown in Figure 3.30. In general, resonance methods can reduce escape times from Earth orbit by over two orders of magnitude vs. using sunlight alone on the sail.[48]

While microwave transmitters have the advantage that they have been under development much longer than lasers and are currently much more efficient and inexpensive to build, they have the disadvantage of requiring much larger apertures for the same focusing distance. This is a significant

disadvantage in missions that require long acceleration times with correspondingly high velocities. However, it can be compensated for with higher acceleration. The ability to operate carbon sails at high temperature enables much higher acceleration, producing large velocities in short distances, thus reducing aperture size. Very low mass probes could be launched from Earth-based microwave transmitters with maximum acceleration achieved over a few hours using apertures only a few hundred meters across.

A number of such missions have been quantified.[49] These missions are for high-velocity mapping of the outer solar system, Kuiper Belt, Plutinos, Pluto and the Heliopause, and the interstellar medium. The penultimate is the interstellar precursor mission. For this mission class, operating at high acceleration, the sail size can be reduced to less than 100 m and an accelerating power of ~100 MW focused on the sail.[50] At 1 GW, sail size extends to 200 m and super-light probes reach velocities of 250 km/sec for very fast missions (see Problem 11).

3.5.3 Deployment of Large Space Structures

Will sails riding beams be stable? The notion of *beam riding*, the stable flight of a sail propelled by a beam, places considerable demands on the sail shape. Even for a steady beam, the sail can wander off if its shape becomes deformed or if it does not have enough spin to keep its angular momentum aligned with the beam direction in the face of perturbations. Beam pressure will keep a concave shape sail in tension, and it will resist side-wise motion if the beam moves off center, as a side-wise force restores it to its position.[51] Experiments have verified that beam riding does occur.[52] Positive feedback stabilization seems effective when the side-wise gradient scale of the beam is the same as the sail concave slope. A broad conical sail shape appears to work best.

Recently, stable beam riding has led to a proposed new type of aircraft/spacecraft, supported from below at altitudes of ~70 km by a radiometric temperature difference effect.[53] An ultralight, mostly carbon fiber "Lifter" is feasible using the radiometric force, an effect known since the 19th century. A powerful microwave beam illuminates the Lifter underside to provide the required temperature difference. Optimally, the full ambient atmospheric pressure can be delivered to one side of the Lifter area by heating it well above the ambient air at 200 K. Beam powers of ~1 MW can support masses of ~100 kg, riding on the narrow microwave beam, and active stabilization is available through beam manipulation. The effect occurs at pressures corresponding to 30 to 150 km altitude, where no aircraft or spacecraft can sustain flight. It can perform communications relay, environmental monitoring, data telemetry, and high-quality optical imaging.

Finally, beams can also carry angular momentum and communicate it to a sail to help control it in flight. Circularly polarized electromagnetic fields carry both energy and angular momentum, which acts to produce a torque through an effective moment arm of a wavelength, so longer wavelengths are more efficient in producing spin. A variety of conducting sail shapes can be spun if they are *not* figures of revolution.

The wave angular momentum imparted to the conducting object scales as wavelength λ. For efficient coupling, λ should be of the order of the sail D_r. This arises because a wave focused to a finite lateral size D generates a component of electric field along the direction of propagation of magnitude λ/D times the transverse electric field, as long as D exceeds the wavelength. The spin frequency S of an object with moment of inertia I grows according to

$$\frac{dS}{dt} = \frac{2P(t)}{I}\frac{\alpha}{\omega} \tag{3.28}$$

where P is the power intercepted by the conductor and α is the absorption coefficient.

Konz and Benford[54] generalized the idea of absorption to include effects arising from the geometric reflection and diffraction of waves, independent of the usual material absorption. They showed that axisymmetric perfect conductors cannot absorb or radiate angular momentum when illuminated. However, any asymmetry allows wave interference effects to produce absorption, even for perfect reflectors, so $\alpha < 0$. Microwaves convey angular momentum at the *edges* of asymmetries because of boundary currents. Such absorption or radiation depends solely on the specific geometry of the conductor. They termed this *geometric absorption*. Conductors can also radiate angular momentum, so their geometric absorption coefficient for angular momentum can even be negative. The geometric absorption coefficient can be as high as 0.5, much larger than typical simple material absorption coefficients, which are typically ~0.1 for absorbers such as carbon and ~0 for conductors. Experiments show the effect is efficient and occurs at very low microwave powers.[55] This effect can be used to stabilize the sail against the drift and yaw, which can cause loss of beam riding, and allows hands-off unfurling deployment through control of the sail spin at a distance.[56]

3.6 Plasma Heating

Controlled thermonuclear fusion promises much as a clean energy source. It has been 50 years in the future for some 50 years now. Nevertheless, progress in fusion parameters of temperature, confinement time, and energy production is slowly moving forward. In the last decade, use of high-average-power microwave beams to heat plasmas to thermonuclear temperatures has expanded greatly. Here we concentrate on electron cyclotron

resonance heating (ECRH) because it is the method receiving the most development. For a detailed description of ion cyclotron resonance heating and lower hybrid heating, consult the first edition. Microwave beams are also used to generate currents in fusion devices (electron cyclotron current drive [ECCD]); we briefly summarize that application.

Both ECRH and ECCD can be highly localized, and therefore are used for toroidal plasma confinement. The applications are stabilization of magnetohydromagnetic instabilities such as tearing notes, production of desirable current density and plasma pressure profiles, and detailed control of plasma energy transport.

For ECCD, electron cyclotron waves drive current in toroidal plasma. A microwave beam launched obliquely into the toroidal plasma excites electrons traveling in one direction. Strong damping of the wave depends upon the velocity direction of the absorbing electrons. These electrons are accelerated to higher energy in that direction, and therefore the current is generated. This method has been widely applied, giving currents of 10 to 100 kA and aiding stabilization of tearing modes in localized regions. For a detailed account of ERCH and ECCD, see Prather's review.[57]

There are three basic microwave heating variants, differing in the frequency of the microwaves that are radiated into the plasma to be resonantly absorbed by the electrons or ions. The three types of heating that have received the most attention and the associated resonant frequencies are as follows:

- Ion cyclotron resonance heating (ICRH)

$$f = f_{ci} = \frac{eB}{2\pi m_i} \tag{3.29}$$

- Lower hybrid heating (LHH)

$$f = f_{LH} \cong \frac{f_{pi}}{\left(1 - \frac{f_{pe}^2}{f_{ce}^2}\right)^{1/2}} \tag{3.30}$$

- Electron cyclotron resonance heating (ECRH)

$$f = f_{ce} = \frac{eB}{2\pi m_e}, \text{ or } f = 2f_{ce} \tag{3.31}$$

where e is the magnitude of the charge on an electron or an ionized isotope of hydrogen, m_i and m_e are the ion and electron masses, B is the magnitude of the local magnetic field, $f_{pe} = (n_e e^2/\varepsilon_0 m_e)^{1/2}/2$, with n_e the volume density of electrons and ε_0 the permittivity of vacuum, and $f_{pi} = (n_i Z_i^2 e^2/\varepsilon_0 m_i)^{1/2}/2$, with $Z_i = 1$ the charge state of the ions in the fusion plasma. At the densities and field values necessary for fusion, $f_{ci} \simeq 100$ MHz, $f_{LH} \simeq 5$ GHz, and $f_{ce} \simeq 140$ to 250 GHz.

The disadvantage of IRCH and LHH frequencies is that it is difficult to design an antenna that efficiently couples the microwaves into a plasma containment vessel with dimensions of the order of the wavelength. In the case of ICRH, there is an added difficulty with coupling the microwaves into the plasma itself, since they must pass through an outer region in the plasma where the waves are attenuated. Overcoming these problems sometimes involves inserting the input antenna into the plasma, which can damage the antenna and inject undesirable impurities into the plasma.

ECRH is now the auxiliary heating method of choice for major fusion devices such as tokamaks and stellerators. Compared to neutral beam heating, ERCH has the advantage of sufficiently high average power to heat plasma in localized regions because of the magnetic field dependence of the mechanism. The other virtue is the ability to place the launching antenna far from the plasma to not perturb or contaminate the fusion experiment. In typical ERCH fusion heating experiments, the gyrotron can be located tens to hundreds of meters from the fusion device and injects into it through small cross-section ports. Both of these virtues are particularly useful in the coming era of major fusion experiments when significant radiation shielding will be required, meaning that small ports are essential and all ancillary equipment must be at some distance.

At the high frequencies and short wavelengths appropriate to ECRH, waves coupling into the plasma and antenna design are much more straightforward. The electron cyclotron wave propagates well in vacuum and couples efficiently to the plasma boundary, in contrast to the other techniques. Additionally, because the magnetic field varies across the plasma, a tunable source could allow selective heating of the plasma at varying depths, and so tailor the density profile of the plasma by taking advantage of the expansion that accompanies a local rise in temperature.

Equation 3.31 shows that ECRH is accomplished at either f_{ce} or $2f_{ce}$. In fact, the choice of frequency depends on the polarization of the microwaves and the point at which they are injected. This can be explained with a rather simple model for the propagation of high-frequency waves in infinite plasma (Figure 3.31); for a more sophisticated treatment, see Ott et al.[58] A uniform magnetic field along the z axis represents the magnetic field confining the plasma. We are interested in waves that will penetrate the confined plasma, so we look at waves propagating across the magnetic field; we designate this direction the x axis, which is the direction of the wavevector, $\mathbf{k} = \hat{x}k$. The microwave fields are represented as plane electromagnetic waves, e.g., $E(x, t) = Ee^{i(kx-\omega t)}$. There are two natural modes of oscillation for the electromagnetic waves in the plasma, depending on the polarization of the electric field vector relative to the magnetic field: